Sensors and Actuators B 185 (2013) 91–96

Contents lists available at SciVerse ScienceDirect

Sensors and Actuators B: Chemical

journal homepage: www.elsevier.com/locate/snb

A symmetrical optical waveguide based surface plasmon resonance biosensing system

Heng Shi[a,1], Zhiyi Liu[a,1], Xiaoxiao Wang[b], Jun Guo[a], Le Liu[a], Lin Luo[c], Jihua Guo[a], Hui Ma[a], Shuqing Sun[a,*], Yonghong He[a,*]

[a] Laboratory of Optical Imaging and Sensing, Graduate School at Shenzhen, Tsinghua University, Shenzhen 518055, China
[b] Life Science Division, Graduate School at Shenzhen, Tsinghua University, Shenzhen 518055, China
[c] Graduate School at Shenzhen, Harbin Institute of Technology, Shenzhen 518055, China

ARTICLE INFO

Article history:
Received 10 January 2013
Received in revised form 28 April 2013
Accepted 1 May 2013
Available online 9 May 2013

Keywords:
Surface plasmon resonance
Symmetrical optical waveguide
Microfluidic system
Dopamine

ABSTRACT

In this work, we propose a MgF_2/Au/MgF_2/Analyte based, angle-interrogation surface plasmon resonance sensor. This symmetrical structure results in higher surface electric field strengths, and longer surface propagation lengths and depths. A refractive index resolution of 8.1×10^{-8} RIU in fluid protocol and 3.5×10^{-7} RIU in atmosphere protocol is acquired by a simple SPR imaging system. In order to demonstrate the biomedical applications of this system, we detect *Escherichia coli* with different concentrations using dopamine film on the sensor surface to immobilize antibodies. A detection limit of 10^3 cfu/mL of *E. coli* bacteria is acquired from this system.

1. Introduction

Surface plasmon resonance (SPR) has continuously been a focus of scientific research, especially in biosensing and chemistry [1–3]. Usually, SPR based sensors exploit the attenuated total reflection (ATR) technique in the frequently used Kretschmann configuration [4], where a thin layer of metal directly deposited on the surface of a prism is scanned with a transverse magnetic beam incident upon its surface at a special angle. The change in the intensity of the reflected beam is then detected to demonstrate the refractive index change of analyte and directly correlated biochemical reactions effect on the sensor surface. SPR sensors offer advantages of direct and label-free detection of biomolecular binding events and typically get a resolution of about 10^{-6} to 10^{-7} refractive index units (RIU) [5]. However, the binding-induced refractive index changes associated with the capture of the bacterial analyte on the surface are extremely small. For this reason, it is necessary to improve the resolution and detection limit in an effort to improve the performance of the sensor. This is why long-range surface plasmon resonance (LRSPR) based sensors are used for improved probing [6].

Long-range surface plasmons (LRSPs) are surface electromagnetic waves that can be produced on thin metallic film imbedded between a buffer medium and the analyte medium with similar refractive indices. Compared with conventional surface plasmons, LRSPs have narrower angular resonance curves, higher surface electric field strengths, and longer surface propagation lengths and depths [7–11]. Due to these advantages, LRSPs have been employed in many fields, such as SP waveguides and biosensors [5,11]. Abbas et al. have discussed the electric field strengths and propagation depth of SPR and SP waveguide [12]. It is reported that an LRSPR based sensor with a refractive index resolution as small as 3×10^{-7} RIU has been demonstrated [13]. However, to support the propagation of the LRSPs, the analyte medium has to show a refractive index close to that of the buffer medium, and therefore only a limited range of refractive index could be detected with high performance. Usually, the full width at half minimum (FWHM) of resonance curve and refractive index resolution for LRSPR are not better than those of conventional SPR when analyte is atmosphere.

Therefore, we intended to further optimize the LRSPR geometry so as to acquire a wider dynamic range maintaining high performance. Through in-depth study of the structure and principles for producing LRSPs, in this paper we propose a symmetrical optical waveguide (SOW) based SPR-supporting biosensing system. Calculation and experiment substantiate that this structure results in better performance than conventional LRSPR no matter fluid or atmosphere analyte. To demonstrate biomedical applications of the SOW based SPR biosensor, we functionalize sensor surface

* Corresponding authors. Tel.: +86 755 26036873; fax: +86 755 26036395.
E-mail addresses: sun.shuqing@sz.tsinghua.edu.cn (S. Sun), heyh@sz.tsinghua.edu.cn (Y. He).

[1] These authors contribute equally to this work.

0925-4005/$ – see front matter © 2013 Elsevier B.V. All rights reserved.
http://dx.doi.org/10.1016/j.snb.2013.05.005

by coating dopamine film and detect *Escherichia coli* with different concentrations using multi-channel microfluidic systems.

2. Materials and methods

2.1. Design consideration

If a thin enough metallic layer is imbedded between two dielectric mediums respectively supporting surface plasmons, the two SPs will couple and exhibit more complex behavior [14]. Specifically, when effective refractive indices of the two mediums are close, the two SPs will form a kind of wave modes referred to as long-range surface plasmons [15]. The closer the two dielectric mediums' refractive indices were, the better performance of LRSPR would be acquired. Usually, the structure supporting LRSPs likes a sandwich, where a thin metallic film imbedded between a buffer medium and the analyte medium with similar refractive indices. Using multiple reflectance theory and Frensnel's formulae [16], the total reflectance is

$$R(\theta) = \left| \frac{r_{12} + r_{234}\ \exp(2i\beta_2)}{1 + r_{12}r_{234}\ \exp(2i\beta_2)} \right|^2, \qquad (1)$$

and

$$r_{234} = \frac{r_{23} + r_{34}\ \exp(2i\beta_3)}{1 + r_{23}r_{34}\ \exp(2i\beta_3)},$$

$$r_{ij} = \frac{n_j\ \cos\ \theta_i - n_i\ \cos\ \theta_j}{n_j\ \cos\ \theta_i + n_i\ \cos\ \theta_j},$$

$$\beta_j = \frac{\omega}{c} d_j \sqrt{\varepsilon_j - \varepsilon_j\ \sin^2\ \theta_j},$$

where the order numbers 1, 2, 3 and 4 represent the prism, buffer layer, metallic film and analyte medium, r_{ij} the reflection coefficient between ith and jth layer and n_i and d_i the refractive index and thickness of the ith layer, respectively. From formula (1), we can see that the LRSPR responses would be best when $\varepsilon_2 = \varepsilon_4$. Therefore, inspired by this, we coated another MgF_2 layer which was the same as the buffer medium onto the metallic film. The structures of conventional LRSPR and SOW based SPR can be seen from Fig. 1a. Finally, theoretical calculations and experiments confirmed our idea. The calculated distribution of electric fields strength were shown in Fig. 1b, where the strength of SOW was approximately three times than that of LRSPR and the depth of electric fields piercing into analyte four times.

2.2. Preparation of sensor chips

Polished SF4 glass substrates were first cleaned with a solution consisting of acetone and ethanol in a 1:1 ratio, dried in a clean air gas stream, then rinsed with deionized water and again dried with nitrogen. The two MgF_2 (magnesium fluoride) layers were deposited by evaporation coating and the thickness were measured by Ellipsometry (M-2000 UI, J.A. Woollam Co. Inc., USA). The gold film was deposited by vacuum magnetron sputtering and the thicknesses were measured with X-ray diffraction (XRD).

2.3. Imaging system

A simple angle-interrogation SPR imaging system was employed. Fig. 2 shows the schematic of our LRSPR imager. In this system, an LED (light emitting diode) with an electric power of 3 W is used as the light source. Emergent light from the integration is parallel with center wavelength of 633 nm. Passing through a polarizer and a cylindrical lens with 50 mm

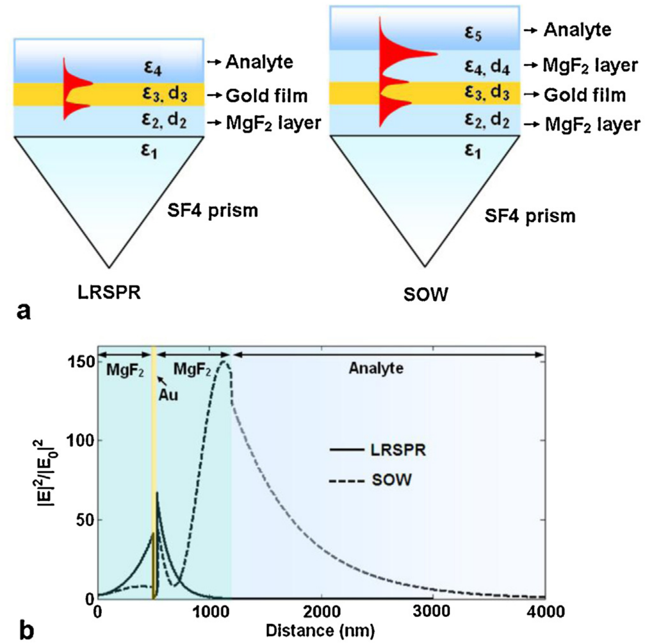

Fig. 1. (a) Structures and distribution of electric fields for two kinds of LRSPR. The thicknesses of Au and MgF_2 layers we used in (b) are as follow: 505 nm MgF_2, 39 nm Au and 645 nm MgF_2. n(SF4) = 1.75, n(MgF_2) = 1.38, n(Au) = 0.197 + 3.09i, n(Analyte) = 1.33.

effective focal length, the light focuses to a line on the surface of sensor chip [17]. In our system, the sensor chip is placed on the surface of a SF4 prism using a droplet of refractive index matching liquid (n = 1.755 RIU, Cargille) to avoid entrapment of air-bubbles. A charge coupled device (CCD, QIMAGING) camera records the images for further data analysis.

2.4. Data analysis

Fig. 3 is demonstration of the data processing. As shown in Fig. 3a, we pumped NaCl (sodium chloride) solutions with different refractive indices into the five channels by a peristaltic pump simultaneously. The refractive indices of NaCl solutions from up to down

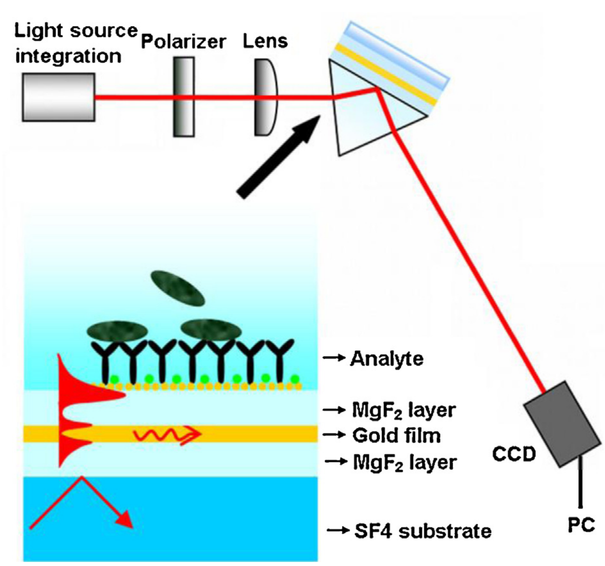

Fig. 2. Schematic of our SOW based SPR imaging system and layers supporting SOW mode.